INTELLIGENT REFLECTING SURFACES ASSISTED FSO AND RF SYSTEMS FOR 5G AND BEYOND WIRELESS COMMUNICATIONS

M.Tech. Thesis

By

SANDESH SHARMA

DEPARTMENT OF ELECTRICAL ENGINEERING

INDIAN INSTITUTE OF TECHNOLOGY INDORE

JUNE 2022

INTELLIGENT REFLECTING SURFACES ASSISTED FSO AND RF SYSTEMS FOR 5G AND BEYOND WIRELESS COMMUNICATIONS

A THESIS

Submitted in partial fulfillment of the requirements for the award of the degree
of
Master of Technology

by

SANDESH SHARMA

DEPARTMENT OF ELECTRICAL ENGINEERING
INDIAN INSTITUTE OF TECHNOLOGY INDORE

JUNE 2022

INDIAN INSTITUTE OF TECHNOLOGY INDORE

CANDIDATE'S DECLARATION

I hereby certify that the work which is being presented in the thesis entitled **INTELLIGENT REFLECTING SURFACES ASSISTED FSO AND RF SYSTEMS FOR 5G AND BEYOND WIRELESS COMMUNICATIONS** in the partial fulfillment of the requirements for the award of the degree of **MASTER OF TECHNOLOGY** and submitted in the **DEPARTMENT OF ELECTRICAL ENGINEERING, Indian Institute of Technology Indore**, is an authentic record of my own work carried out during the time period from August 2020 to June 2022 under the supervision of **Dr. Swaminathan Ramabadran, Assistant Professor at Indian Institute of Technology Indore**.

The matter presented in this thesis has not been submitted by me for the award of any other degree of this or any other institute.

S sharma 01/06/2022

Signature of the student with date
SANDESH SHARMA

This is to certify that the above statement made by the candidate is correct to the best of my/our knowledge.

01/06/2022
Signature of the Supervisor of M.Tech. thesis (with date)
Dr. SWAMINATHAN RAMABADRAN

SANDESH SHARMA has successfully given his/her M.Tech. Oral Examination held on **07/06/2022**.

Signature(s) of Supervisor(s) of M.Tech. thesis
Date: 07/06/2022

Convener, DPGC
Date: 07/06/2022

Saptarshi Ghosh
Signature of PSPC Member #1
Date: 07/06/2022

Signature of PSPC Member #2
Date: 07-06-2022

Acknowledgments

Firstly, I would like to express my sincere gratitude to my supervisor Dr. Swaminathan R. for his continuous support and valuable guidance. His guidance helped me in throughout my work. I have been able to push myself beyond my expectations with his excellent supervision and encouragement.

I would like to thank my PSPC members Dr. Saptarshi Ghosh and Dr. Antony Vijesh for their insightful comments and suggestions towards my research.

I would also like to thank my colleagues at lab Mr. Narendra Vishwakarma, Ms. Deepshikha Singh, and Mr. Aravind Marrapu for some valuable suggestions whenever I was stuck.

I sincerely acknowledge IIT Indore and Ministry of Education, Govt. of India, for supporting my M.Tech. by providing lab facilities and TA scholarship, respectively.

Last but not the least, my work would not have been possible without the encouragement of my parents, whose tremendous support helped me stay positive and overcome the worst of hurdles. To them, I will forever be grateful.

Abstract

With possible new use cases and hard needs of upcoming 5th generation (5G) and beyond wireless networks, the future of mobile communications appears intriguing. The propagation medium has been regarded as a randomly behaving entity between the transmitter and the receiver since the dawn of the modern era of wireless communications, degrading the quality of the received signal due to the uncontrollable interactions of the transmitted radio waves with the surrounding objects. On the other hand, the recent introduction of intelligent reflecting surfaces (IRS) in wireless communications allows network operators to adjust the scattering, reflection, and refraction properties of radio waves, therefore eliminating the detrimental impacts of natural wireless propagation.

IRS has recently demonstrated that it can successfully regulate the wavefront of incoming signals, including phase, amplitude, frequency, and even polarization, without the use of sophisticated decoding, encoding, and radio frequency processing methods. The IRS is a viable alternative to active reliance techniques for improving the performance of wireless systems without requiring extensive processing at the relay. In addition to this, free space optics (FSO) communication is a promising solution for high-data-rate transmission over a large bandwidth in the optical spectrum without requiring a license. The FSO operates in above 300 GHz (Infrared, Ultraviolet) range and is an emerging alternative to radio frequency (RF) communication.

Free space optics (FSO) communication is seen as a cost-effective way to provide higher bandwidth, higher data rates, better link security, higher immunity to interference, etc., compared to radio frequency (RF) communication over short link distances. Despite these advantages, FSO link is severely affected by pointing errors, atmospheric turbulence, and signal loss due to the obstructions caused by buildings, trees, mountains, etc. In our work, we propose a hybrid and a mixed communication system model consisting of a FSO subsystem and a RF subsystem with the goal to improve the coverage and system reliability. In addition,

both the FSO and RF subsystems are assisted by intelligent reflecting surfaces (IRS). Specifically, we carry out the performance analysis of the IRS-assisted hybrid FSO/RF system and IRS-assisted mixed FSO/RF system by deriving closed-form expressions for various performance metrics. The derived performance metrics have been validated using Monte-Carlo simulations. Finally, numerical results are shown along with insightful discussions.

Contents

List of Figures

Chapter 1

Introduction

1.1 Introduction

Recent introduction of intelligent reflecting surfaces (IRS) is a completely different concept [1]. Since the beginning of the modern communication, the wireless medium has been considered as a randomly behaving entity between transmitter and receiver, which degrades the quality of received signal. The IRS are made up of man-made electromagnetic materials, which can be used to intelligently control the electromagnetic properties of the incident waves, such as phase, angle of reflection, amplitude, and polarization [2] to improve the signal quality at the receiver. IRS is also referred to as reconfigurable intelligent surfaces (RIS), large intelligent surfaces (LIS), intelligent wall (IW), etc. The significant advantages of IRS include very low power consumption, enhanced coverage area, and improved link reliability over competing wireless technologies like cooperative relay systems [3].

Also due to the increasing number of wireless multimedia devices and new applications, there is always a requirement of ultra-high bandwidth, high data rates, high-speed backhaul networks, high security, low latency, improved reliability, etc. Though the fifth-generation (5G) wireless communication technologies are capable of addressing few of these requirements, there is still a great challenge to fulfill most of the requirements of future-generation wireless systems after ten years. This has motivated the researchers to work towards sixth-generation (6G) wireless communication systems [4]. Since radio frequency (RF) spectrum is capacity limited as well as congested, it is essential to look for alternative solutions. One possible solution is to tap much wider optical spectrum near infrared (IR) band. Free space optics (FSO) communication operates in near IR band and it provides higher capacity, higher bandwidth, higher immunity to interference, better link security, etc., compared to RF communication as well as very cost-effective due to unlicensed spectrum. Thus, FSO communication is considered as a promising technology for providing high-capacity wireless backhaul connectivity in 6G [5].

Despite various advantages of FSO communication, the link performance is undermined by the atmospheric turbulence, pointing errors, and atmospheric attenuation. In order to improve the reliability of the FSO communication system, an additional RF subsystem was used as a backup for the FSO subsystem and this led to the development of hybrid FSO/RF system. Another way to improve performance is by combining FSO and RF in a dual-hop scenario which is mixed FSO/RF system.

The hybrid and mixed FSO/RF system are used to take advantages of both FSO and RF technologies simultaneously. However, obstruction between the transmitter and the receiver because of buildings, trees, mountains, etc., can still affect the transmission. So, integrating IRS with such systems would be a promising scenario for 5G and beyond communication.

1.2 Literature Review

Recently, many research works have been done by integrating IRS with various technologies. In [3], the average symbol error probability (SEP) performance of an IRS-assisted RF system was investigated, where the small-scale fading in the RF link was modeled using Rayleigh distribution. In [6], the performance of a terrestrial FSO system assisted using a single-element IRS was analyzed and the exact closed-form expressions for probability density function (PDF), cumulative distribution function (CDF), moment generating function (MGF), outage probability, channel capacity, and average bit error rate (BER) were derived. They used IRS to intentionally modify the phase of the incident signals to improve the signal quality at the receiver.

Authors in [7] have analysed the performance in terms of outage probability, average symbol error rate, and ergodic channel capacity for the IRS-assisted single link FSO system. In addition, Gamma-Gamma distribution was considered for atmospheric turbulence model and pointing errors due to beam jitter were also considered. In [8], the performance analysis in terms of outage probability, average BER, and channel capacity of an IRS-assisted multiple link FSO system was carried out. Further, the atmospheric turbulence-induced fading in the FSO link was modeled using Gamma-Gamma distribution and the effects of pointing errors due to beam jitter and IRS jitter on the system performance were also taken into consideration. Multiple transmitter and receiver apertures were considered and each transmitter aperture sends the signal to individual receiver aperture through an IRS element and the all received signals were combined using maximal ratio combining (MRC) technique.

To improve the performance of FSO communication systems other than using IRS, authors in [9] have done a comprehensive performance analysis of a terrestrial hybrid FSO/RF system was carried out assuming a hard-switching scheme, where either FSO or RF link will be activated at a particular instant of time. Further, performance improvement techniques such as maximal ratio combining (MRC), selection combining (SC), etc., for hybrid FSO/RF system were analyzed in [10]. In [11], The authors have analysed the performance of dual-hop FSO/RF transmission systems with amplify-and-forward (AF) fixed relaying technique in terms of outage probability, average BER and ergodic capacity. In [12], IRS was integrated with RF link in mixed FSO/RF system and further enhancements from mixed FSO/RF system in performance metrics were analysed.

1.3 Motivations and Contributions

1.3.1 Chapter 2

The motivations behind the work in Chapter 2 are summarized as follows:

- The performance of IRS-assisted hybrid FSO/RF system has not been investigated in the existing literature to the best of our knowledge.
- In hybrid FSO/RF system, the reliability of system is improved because of the RF link as a backup in different weather conditions, but system performance is affected due to obstructions between the transmitter and the receiver.
- In the IRS-assisted FSO system, the system is immune from the obstruction but the reliability is the main problem.
- The IRS-assisted hybrid FSO/RF system compensates the problem of reliability as well as obstructions.

The contributions of the work in Chapter 2 are summarized as follows:

- The closed-form expressions for performance metrics such as outage probability, average BER, and ergodic capacity of the proposed system model are derived.
- The Monte Carlo simulations are also carried out to validate the derived closed-form expressions.
- Average BER and ergodic capacity of the IRS-assisted hybrid FSO/RF system are compared to other FSO-based systems.
- Effects of increasing number of IRS elements and beam jitter deviation are also analysed.

1.3.2 Chapter 3

The motivations behind the work in Chapter 3 are summarized as follows:

- The existing literature has analysed the mixed FSO/RF systems with IRS used in the RF link only.
- IRS when used with both FSO and RF can compensates the obstruction between both the links and improves the coverage of the system.
- Performance analysis of IRS with FSO over Malaga fading channel has not been done to the best of our knowledge.

The contributions of the work in Chapter 3 are summarized as follows:

- The closed-form expressions for outage probability and average BER of the proposed system model are derived.
- Malaga fading channel is considered for FSO subsystem and Rayleigh fading is considered for RF subsystem.
- The Monte Carlo simulations are also carried out to validate the derived closed-form expressions.
- Average BER and outage probability of the IRS-assisted mixed FSO/RF system are compared to other FSO-based systems.
- Effects of pointing errors and atmospheric turbulence on system performance is analysed.

1.4 Organization of the Thesis

The rest of this thesis is organized as follows: In Chapter 2, performance analysis of the IRS-assisted hybrid FSO/RF system is discussed. Further, in Chapter 3, performance analysis of the IRS-assisted mixed FSO/RF system is carried out. Finally, Chapter 4 includes the conclusion and scope of the future work of this thesis.

Chapter 2

Performance Analysis of IRS-Assisted Hybrid FSO/RF Communication System

2.1 Introduction

This chapter describes an IRS-assisted hybrid FSO/RF system model. In the proposed system model, we considered one source, two IRSs and one destination. The source consists of multiple aperture FSO transmitter and a backup RF transmitter. Similarly, the destination has multiple aperture FSO receiver and a backup RF receiver. The IRS for FSO subsystem consists of N_f reflector elements and IRS for RF subsystem consists of N_r reflector elements. Further, we assume that there is no direct line-of-sight (LoS) path between the source and destination, and hence, IRS is used to create a virtual LoS path. It is also assumed that the receiver has the perfect channel state information (CSI). The priority to send message signal is given to FSO subsystem, in which multiple apertures send message signal via N_f reflecting elements. Now those message signals can be combined using various diversity combining techniques such as switched combining, equal-gain combining, selection combining, maximal ratio combining (MRC). In our work, we have used MRC technique. A weighted summation of signals is conducted in the MRC approach, with amplitudes proportional to signal-to-noise ratio (SNR) for each signal and phase kept equal. We have assumed a single-threshold-based switching to switch between FSO and RF subsystem. The RF subsystem will only be active when the instantaneous SNR of FSO subsystem falls below a certain threshold SNR value, denoted as γ_{th}. Under such conditions, FSO will remain inactive and message signal will only be transmitted through IRS-assisted RF subsystem. The performance of the proposed system is analyzed by deriving the outage probability, average BER, and ergodic capacity expressions.

2.2 Organisation of Chapter

The rest of the chapter is organized as follows: The system model for IRS-assisted hybrid FSO/RF system has been discussed in Section 2.3. Section 2.4 provides the closed-form expressions for outage probability, average BER, and ergodic capacity. Furthermore, Numerical results and inferences are given in Section 2.5. Finally, the concluding remarks are given in Section 2.6.

2.3 System Model

We consider an IRS-assisted hybrid FSO/RF communication system, shown in Figure 2.1. In normal condition, the IRS-assisted FSO (IAFSO) subsystem is sending signal to receiver through N_f links. When the instantaneous SNR of the IAFSO subsystem falls below the threshold SNR, γ_{th}, the IAFSO subsystem will stop sending signal and the IRS-assisted RF (IARF) subsystem will start sending the message signal. This decision is taken based on 1-bit feedback signal from the receiver. We consider sub-carrier intensity modulation (SIM) for FSO subsystem with binary phase-shift-keying (BPSK) scheme at the transmitter and direct detection (DD) technique is assumed for detecting the FSO signals at the receiver. Moreover, we consider BPSK scheme for the RF subsystem at the transmitter and a coherent detection technique at the receiver. The main assumptions considered in our work are as follows: The channel state information (CSI) is assumed to be perfectly available at the receiver for both FSO and RF subsystems. Furthermore, the 1-bit feedback signal received for switching between FSO and RF subsystems is assumed to be received without any error.

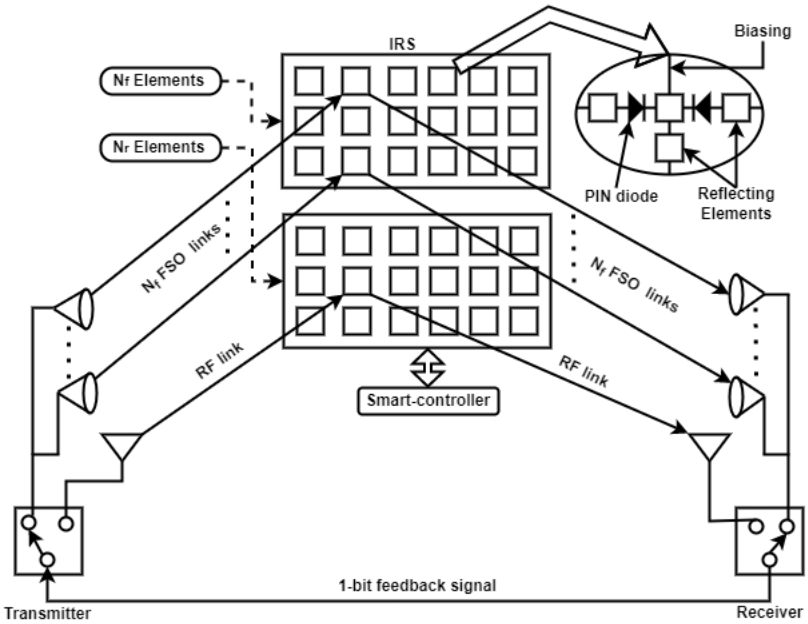

Figure 2.1: System model for IRS-assisted hybrid FSO/RF communication system

2.3.1 FSO Channel Model

There are N_f FSO links in IAFSO subsystem and for any k^{th} link, where $k \in \{1,2,...,N_f\}$, the main signal impairments in FSO considered are atmospheric turbulence, h_{ak} and pointing errors, h_{pk}.

Atmospheric Turbulence Model:

For any k^{th} link, the end-to-end atmospheric turbulence is the cascaded turbulence from source to k^{th} reflector and from k^{th} reflector to destination given as

$$h_{ak} = h_{ak_1} h_{ak_2} \tag{2.1}$$

where h_{ak_1} and h_{ak_2} denote the atmospheric turbulence-induced fading coefficients from transmitter to k^{th} IRS element and k^{th} IRS element to receiver, respectively. Let $L_{1,k}$ and $L_{2,k}$ denote the distances from transmitter to IRS and from IRS to receiver, respectively. Further, we assume $L_{1,k} = L_{2,k} = L$ by considering the far-field case. The moderate-to-strong atmospheric turbulence encountered by the FSO links can be modeled using Gamma-Gamma distribution and the probability density function (PDF) is given by [13, Eq.(12)]

$$f_{h_{ak_i}}(x) = \frac{2(\alpha\beta)^{\frac{\alpha+\beta}{2}}}{\Gamma(\alpha)\Gamma(\beta)} x^{\frac{\alpha+\beta}{2}-1} K_{\alpha-\beta}(2\sqrt{\alpha\beta x}) \qquad i \in \{1,2\} \tag{2.2}$$

where $\alpha > 0$ and $\beta > 0$ represent the large scale and small scale scattering parameters, respectively and $K_v(\cdot)$ is the v^{th}-order modified Bessel function of second kind [14, Eq. (8.407)]. The PDF of end-to-end atmospheric turbulence can be derived by solving the integral given by

$$f_{h_{ak}}(x) = \int_0^\infty f_{h_{ak_1}}(t) f_{h_{ak_2}}\left(\frac{x}{t}\right)\frac{1}{t}dt \tag{2.3}$$

After substituting (2.2) in (2.3), we get

$$f_{h_{ak}}(x) = \left(\frac{2(\alpha\beta)^{\frac{\alpha+\beta}{2}}}{\Gamma(\alpha)\Gamma(\beta)}\right)^2 x^{\left(\frac{\alpha+\beta}{2}-1\right)} \int_0^\infty t^{-1} K_{\alpha-\beta}(2\sqrt{\alpha\beta t}) K_{\alpha-\beta}\left(2\sqrt{\alpha\beta\frac{x}{t}}\right) dt \tag{2.4}$$

The integral is solved by writing modified Bessel function of second kind in the form of another special function named Meijer-G function [15, Eq. (03.04.26.0008.01)]. After that, using [15, Eq. (07.34.17.0012.01)] and [15, Eq. (07.34.21.0011.01)] to obtain the PDF of end-to-end atmospheric turbulence for the k^{th} link as

$$f_{h_{ak}}(x) = \left(\frac{(\alpha\beta)^{\frac{\alpha+\beta}{2}}}{\Gamma(\alpha)\Gamma(\beta)}\right)^2 x^{\left(\frac{\alpha+\beta}{2}-1\right)} G_{0\,4}^{4\,0}\left((\alpha\beta)^2 x \,\middle|\, \begin{matrix} - \\ \frac{\alpha-\beta}{2}, \frac{\beta-\alpha}{2}, \frac{\alpha-\beta}{2}, \frac{\beta-\alpha}{2} \end{matrix}\right) \tag{2.5}$$

where $G_{:}^{:}\left(\cdot\middle|\cdot\right)$ denotes the Meijer G-function [15, Eq.(07.34.02.0001.01)].

Pointing Error Model:

The pointing errors in the IRS-assisted FSO system are mainly due to beam jitter and IRS jitter [8], where the beam jitter is caused by the vibrations of the transmitter and IRS jitter refers to the normal vector deflection caused by the vibrations of the reflecting surface. The end-to-end pointing error for the k^{th} link is approximately given by [16]

$$h_{pk} \approx A_0 \exp\left(-\frac{2r^2}{w_{zeq}}\right) \tag{2.6}$$

where r is the radial displacement caused by beam and IRS jitter, A_0 represents the fraction of power at the receiver aperture, and w_{zeq} is the equivalent beam width. Further, A_0 and w_{zeq} can be calculated as

$$A_0 = \text{erf}^2(v) \tag{2.7}$$

$$w_{zeq}^2 = w_z^2 \frac{\sqrt{\pi}\text{erf}(v)}{2ve^{-v^2}} \tag{2.8}$$

where $\text{erf}(\cdot)$ denotes the error function [14, Eq. (8.25)]. Further, $v = \sqrt{\frac{\pi}{2}}\frac{a}{w_z}$, where a is the aperture radius and w_z is the beam width. The PDF of the end-to-end pointing error for the

k^{th} is given by

$$f_{h_{pk}}(x) = \frac{c}{A_0}\left(\frac{x}{A_0}\right)^{c-1}, 0 < x < A_0, \tag{2.9}$$

where c is the pointing error coefficient and is given by

$$c = \frac{w_{zeq}^2}{16(\sigma_\theta^2 L^2 + \sigma_\beta^2 L^2)} \tag{2.10}$$

σ_θ and σ_β here are the standard deviations of beam and IRS jitter, respectively.

Combined Channel Model:

The combined channel irradiance for the k^{th} link is the product of atmospheric turbulence and pointing errors, and is given by

$$h_k = h_{ak} h_{pk} \tag{2.11}$$

The PDF of the combined channel irradiance for k^{th} is obtained by solving the integral

$$f_{h_k}(x) = \int_{\frac{x}{A_0}}^{\infty} f_{h_{ak}}(t) f_{h_{pk}}\left(\frac{x}{t}\right)\frac{1}{t}dt \tag{2.12}$$

After substituting (2.5) and (2.9) in (2.12) and simplifying, we obtain

$$f_{h_k}(x) = \left(\frac{(\alpha\beta)^{\frac{\alpha+\beta}{2}}}{\Gamma(\alpha)\Gamma(\beta)}\right)^2 \left(\frac{cx^{(c-1)}}{A_0^c}\right) \int_{\frac{x}{A_0}}^{\infty} t^{\left(\frac{\alpha+\beta}{2}-c-1\right)} G_{0\,4}^{4\,0}\left((\alpha\beta)^2 x \middle| \begin{matrix} - \\ \frac{\alpha-\beta}{2}, \frac{\beta-\alpha}{2}, \frac{\alpha-\beta}{2}, \frac{\beta-\alpha}{2} \end{matrix}\right) dt \tag{2.13}$$

Using [15, Eq. (07.34.21.0085.01)] and [15, Eq. (07.34.17.0011.01)], the integral is solved and PDF is given as

$$f_{h_k}(x) = \left[\frac{cx^{-1}}{(\Gamma(\alpha)\Gamma(\beta))^2}\right] G_{1\,5}^{5\,0}\left(\frac{(\alpha\beta)^2 x}{A_0} \middle| \begin{matrix} c+1 \\ c, \alpha, \beta, \alpha, \beta \end{matrix}\right) \tag{2.14}$$

Instantaneous SNR:

The instantaneous SNR of the k^{th} FSO link γ_{FSO_k}, is given by

$$\gamma_{FSO_k} = \overline{\gamma}_{FSO} h_k^2 \tag{2.15}$$

where $\overline{\gamma}_{FSO}$ denotes the average SNR and h_k represents the combined channel state of the k^{th} FSO link. Further, the overall instantaneous SNR can be obtained by applying the MRC technique and is formulated as

$$\gamma_{FSO} = \sum_{k=1}^{N_f} \gamma_{FSO_k} = \overline{\gamma}_{FSO} \sum_{k=1}^{N_f} h_k^2 \tag{2.16}$$

Using the power transformation of the random variable, the PDF of $Z = h_k^2$ can obtained as

$$f_Z(x) = \left[\frac{cx^{-1}}{2(\Gamma(\alpha)\Gamma(\beta))^2}\right] G_{1\,5}^{5\,0}\left(\frac{(\alpha\beta)^2\sqrt{x}}{A_0}\middle|\begin{matrix}1+c\\ c,\alpha,\beta,\alpha,\beta\end{matrix}\right) \tag{2.17}$$

Now, we obtain mean μ_1 of Z as

$$\begin{aligned}\mu_1 = E[Z] &= \int_0^\infty x f_Z(x)dx \\ &= \int_0^\infty \left[\frac{c}{2(\Gamma(\alpha)\Gamma(\beta))^2}\right] G_{1\,5}^{5\,0}\left(\frac{(\alpha\beta)^2\sqrt{x}}{A_0}\middle|\begin{matrix}1+c\\ c,\alpha,\beta,\alpha,\beta\end{matrix}\right) dx\end{aligned} \tag{2.18}$$

where $E[\cdot]$ denotes the expected value. The above integral is solved using [15, Eq. (07.34.21.0009.01)] and mean is given as

$$\mu_1 = \frac{cA_0^2(\Gamma(\alpha+2)\Gamma(\beta+2))^2}{(c+2)(\Gamma(\alpha)\Gamma(\beta))^2(\alpha\beta)^4} \tag{2.19}$$

Similarly, we solve for variance Ω_1^2 and obtain

$$\Omega_1^2 = E[Z^2] - (E[Z])^2 = \frac{cA_0^4(\Gamma(\alpha+4)\Gamma(\beta+4))^2}{(c+4)(\Gamma(\alpha)\Gamma(\beta))^2(\alpha\beta)^8} - \mu_1^2 \tag{2.20}$$

From (2.15) and (2.17), we get the PDF of instantaneous SNR γ_{FSO_k} for the k^{th} link as

$$f_{\gamma_{FSO_k}}(x) = \frac{cx^{-1}}{2(\Gamma(\alpha)\Gamma(\beta))^2} G_{1\,5}^{5\,0}\left(\frac{(\alpha\beta)^2\sqrt{x}}{A_0\sqrt{\overline{\gamma}_{FSO}}}\middle|\begin{matrix}1+c\\ c,\alpha,\beta,\alpha,\beta\end{matrix}\right) \tag{2.21}$$

However, it is difficult to evaluate the PDF of overall instantaneous SNR γ_{FSO} using (2.21). Hence, by assuming a large N_f and applying the central limit theorem (CLT) [17], the PDF of γ_{FSO} can be well approximated using a Gaussian random variable with mean $\mu = \overline{\gamma}_{FSO} \times \mu_1 \times N_f$ and variance $\Omega^2 = \overline{\gamma}_{FSO}^2 \times \Omega_1^2 \times N_f$. Therefore, the PDF of γ_{FSO} can be written as

$$f_{\gamma_{FSO}}(x) \approx \frac{1}{\sqrt{2\pi\Omega^2}} e^{-\frac{(x-\mu)^2}{2\Omega^2}} \tag{2.22}$$

Further, we can use (2.22) to obtain the CDF of γ_{FSO} as

$$F_{\gamma_{FSO}}(x) \approx \frac{1}{2}\left[\operatorname{erf}\left(\frac{x-\mu}{\sqrt{2}\Omega}\right) - \operatorname{erf}\left(-\frac{\mu}{\sqrt{2}\Omega}\right)\right] \tag{2.23}$$

2.3.2 RF Channel Model

The IRS-assisted RF channel is modeled using two cascaded channels, i.e. transmitter to IRS and IRS to receiver. Let b_i and g_i denote the small-scale fading channel coefficients between transmitter and i^{th} reflector and i^{th} reflector and receiver, respectively. We assume that the RF channel encounters slow and flat fading and it is modeled using the Rayleigh distribution, i.e. $b_i, g_i \sim \mathscr{CN}(0,1)$, where $\mathscr{CN}(0, \sigma^2)$ denotes the complex Gaussian distribution with zero-mean and variance σ^2. The collective RF channel in case of IRS-assisted RF subsystem is given by $H_i = b_i e^{j\phi_i} g_i$, where ϕ_i is the adjustable phase of i^{th} reflector, $b_i = \chi_i e^{-j\theta_i}$ and $g_i = \zeta_i e^{-j\psi_i}$ are given in terms of channel amplitudes χ_i and ζ_i and phases θ_i and ψ_i. Thus, the instantaneous SNR at the receiver can be calculated as [18]

$$\gamma_{RF} = \frac{\left|\sum_{i=1}^{N_r} H_i\right|^2 E_s}{N_0} = \left|\sum_{i=1}^{N_r} \chi_i \zeta_i e^{j(\phi_i - \theta_i - \psi_i)}\right|^2 \overline{\gamma}_{RF} \tag{2.24}$$

where $\overline{\gamma}_{RF} = \frac{E_s}{N_0}$ is the average SNR of the RF link. Further, the RF channel phases can be eliminated by adjusting the IRS phase as $\phi_i = \theta_i + \psi_i$ to obtain the maximized instantaneous SNR, which is expressed as

$$\gamma_{RF} = \left|\sum_{i=1}^{N_r} \chi_i \zeta_i\right|^2 \overline{\gamma}_{RF} = B^2 \overline{\gamma}_{RF} \tag{2.25}$$

where χ_i and ζ_i are independent Rayleigh distributed random variables and the mean and variance of their product are given by $\mathrm{E}[\chi_i\zeta_i] = \frac{\pi}{4}$ and $\mathrm{VAR}[\chi_i\zeta_i] = \left(1 - \frac{\pi^2}{16}\right)$, respectively. By assuming a large N_r and applying CLT, B follows Gaussian distribution with mean and variance $\mathrm{E}[B] = \frac{N_r \pi}{4}$ and $\mathrm{VAR}[B] = N_r\left(1 - \frac{\pi^2}{16}\right)$, respectively. Since B follows Gaussian distribution, γ_{RF}, which is proportional to B^2 as observed in (2.25), will follow a non-central chi-square distribution with one degree of freedom and its PDF is given by [17]

$$f_{\gamma_{RF}}(\gamma) = \frac{1}{2\delta^2}\left(\frac{\gamma}{\lambda}\right)^{-\frac{1}{4}} \exp\left(-\frac{\gamma+\lambda}{2\delta^2}\right) \mathrm{I}_{-\frac{1}{2}}\left(\frac{\sqrt{\gamma\lambda}}{\delta^2}\right) \tag{2.26}$$

where $\lambda = \frac{\overline{\gamma}_{RF}\pi^2 N_r^2}{16}$, $\delta^2 = \frac{\overline{\gamma}_{RF}(16-\pi^2)N_r}{16}$, and $\mathrm{I}_{-\frac{1}{2}}(\cdot)$ denotes the modified Bessel function of the first kind [17, Eq.(2.3–31)]. From (2.26), we can obtain the CDF of γ_{RF} as

$$F_{\gamma_{RF}}(\gamma) = 1 - Q_{\frac{1}{2}}\left(\frac{\sqrt{\lambda}}{\delta}, \frac{\sqrt{\gamma}}{\delta}\right) \tag{2.27}$$

where $Q_m(j,k)$ is the Marcum Q-function [17, Eq. (2.3-36)].

2.4 Performance Analysis

2.4.1 Outage Probability Analysis

The IRS-assisted hybrid FSO/RF system will be in outage if both the FSO and RF subsystems will be in outage. The end-to-end outage probability of the IRS-assisted hybrid FSO/RF system can be expressed as

$$P_{out} = \Pr(\gamma_{FSO} < \gamma_{th} \text{ and } \gamma_{RF} < \gamma_{th}) = F_{\gamma_{FSO}}(\gamma_{th}) \times F_{\gamma_{RF}}(\gamma_{th}) \tag{2.28}$$

where γ_{th} is the outage threshold SNR value. We can obtain $F_{\gamma_{FSO}}(\gamma_{th})$ and $F_{\gamma_{RF}}(\gamma_{th})$ from (2.23) and (2.27), respectively. Finally, the overall outage probability can be expressed as

$$P_{out} = \frac{1}{2}\left[\operatorname{erf}\left(\frac{\gamma_{th}-\mu}{\sqrt{2}\Omega}\right) - \operatorname{erf}\left(-\frac{\mu}{\sqrt{2}\Omega}\right)\right]\left[1 - Q_{\frac{1}{2}}\left(\frac{\sqrt{\lambda}}{\delta}, \frac{\sqrt{\gamma_{th}}}{\delta}\right)\right] \tag{2.29}$$

2.4.2 Average BER

The average BER P_e^H of the IRS-assisted hybrid FSO/RF system based on the hard-switching scheme is given by [9]

$$P_e^H = B_{FSO}(\gamma_{th}) + F_{\gamma_{FSO}}(\gamma_{th}) P_e^{RF} \tag{2.30}$$

where B_{FSO} represents the average BER during the non-outage period of the FSO subsystem and P_e^{RF} represents the average BER of the RF subsystem. The average BER of the FSO subsystem during the non-outage period for BPSK modulation scheme can be calculated as [17]

$$B_{FSO}(\gamma_{th}) = \int_{\gamma_{th}}^{\infty} Q(\sqrt{2\gamma}) f_{\gamma_{FSO}}(\gamma) d\gamma, \tag{2.31}$$

where $Q(\sqrt{2\gamma})$ indicates the conditional error probability of BPSK signalling and $Q(\cdot)$ denotes the Q-function [14, Eq. (6.287.3)]. Further, from [19, Eq. (14)] and [14, Eq. (6.287)], Q-function can be approximated as

$$Q(x) = \frac{1}{2}\operatorname{erfc}\left(\frac{x}{\sqrt{2}}\right) \simeq \frac{1}{12}e^{-\frac{x^2}{2}} + \frac{1}{4}e^{-\frac{2x^2}{3}} \tag{2.32}$$

Substituting (2.22) and (2.32) in (2.31), we get

$$B_{FSO}(\gamma_{th}) \simeq \int_{\gamma_{th}}^{\infty} \left(\frac{1}{12}e^{-\frac{\gamma^2}{2}} + \frac{1}{4}e^{-\frac{2\gamma^2}{3}}\right) \frac{1}{\sqrt{2\pi\Omega^2}} e^{-\frac{(\gamma-\mu)^2}{2\Omega^2}} d\gamma \tag{2.33}$$

Using [14, Eqs. (2.322.1) and (2.322.2)], the integral is evaluated as

$$B_{FSO}(\gamma_{th}) \simeq \frac{1}{12}e^{\left(\frac{\Omega^2}{2}-\mu\right)} Q\left(\frac{\gamma_{th}+\Omega^2-\mu}{\Omega}\right) + \frac{1}{4}e^{\left(\frac{8\Omega^2}{9}-\frac{4\mu}{3}\right)} Q\left(\frac{\gamma_{th}+\frac{4}{3}\Omega^2-\mu}{\Omega}\right) \tag{2.34}$$

For the IRS-assisted RF subsystem, we can obtain the average BER of BPSK signaling from moment generating function (MGF) as [20]

$$P_e^{RF} = \frac{1}{\pi}\int_0^{\frac{\pi}{2}} M_{\gamma_{RF}}\left(\frac{-1}{\sin^2\eta}\right)d\eta, \tag{2.35}$$

where $M_{\gamma_{RF}}(s)$ is the MGF of γ_{RF} given as

$$M_{\gamma_{RF}}(s) = \sqrt{\frac{1}{1-\frac{sN_r\left(16-\pi^2\right)E_s}{8N_0}}}\exp\left(\frac{\frac{sN_r^2\pi^2E_s}{16N_0}}{1-\frac{sN_r\left(16-\pi^2\right)E_s}{8N_0}}\right) \tag{2.36}$$

After substituting $M_{\gamma_{RF}}(s)$, the expression in (2.35) can rewritten as

$$P_e^{RF} = \frac{1}{\pi}\int_0^{\frac{\pi}{2}}\left(\frac{1}{1+\frac{N_r(16-\pi^2)E_s}{8\sin^2\eta N_0}}\right)^{\frac{1}{2}}\exp\left(\frac{\frac{-N_r^2\pi^2E_s}{16\sin^2\eta N_0}}{1+\frac{N_r(16-\pi^2)E_s}{8\sin^2\eta N_0}}\right)d\eta \tag{2.37}$$

Further, to gain more insights on the average BER performance of the RF subsystem, (2.37) can be upper bounded by letting $\eta = \frac{\pi}{2}$ as

$$P_e^{RF} \le \frac{1}{2}\left(\frac{1}{1+\frac{N_r\left(16-\pi^2\right)E_s}{8N_0}}\right)^{\frac{1}{2}}\exp\left(\frac{-\frac{N_r^2\pi^2E_s}{16N_0}}{1+\frac{N_r\left(16-\pi^2\right)E_s}{8N_0}}\right) \tag{2.38}$$

2.4.3 Ergodic Channel Capacity

The ergodic channel capacity of the IRS-assisted hybrid FSO/RF system is given by

$$C_{hyb} = C_{FSO}(\gamma_{th}) + F_{\gamma_{FSO}}(\gamma_{th})C_{RF} \tag{2.39}$$

where $C_{FSO}(\gamma_{th})$ is the ergodic channel capacity of the IRS-assisted FSO subsystem under non-outage period and C_{RF} is the ergodic channel capacity of the IRS-assisted RF subsystem. The ergodic channel capacity of the FSO subsystem under non-outage period is given by

$$C_{FSO}(\gamma_{th}) = \int_{\gamma_{th}}^{\infty}\log_2(1+x)f_{\gamma_{FSO}}(x)dx \tag{2.40}$$

By utilizing [21], the logarithm function can be well-approximated as

$$\log_2(1+x) \approx \sum_{i=1}^{4}\eta_i e^{-\xi_i x} \tag{2.41}$$

where $\eta_i = [9.331, -2.635, -4.032, -2.388]$ and $\xi_i = [0.000, 0.037, 0.004, 0.274]$. After applying the approximation in (2.40), substituting the value of $\gamma_{FSO}(x)$, and simplifying, the integral becomes

$$C_{FSO}(\gamma_{th}) = \sum_{i=1}^{4}\eta_i\int_{\gamma_{th}}^{\infty}\frac{1}{\sqrt{2\pi\Omega^2}}\exp\left[-\left(\xi_i x + \frac{(x-\mu)^2}{2\Omega^2}\right)\right]dx \tag{2.42}$$

Evaluating the integral using Q-function, the final expression for channel capacity is given by

$$C_{FSO}(\gamma_{th}) \approx \sum_{i=1}^{4} \eta_i e^{\xi_i \left(\frac{\xi_i \Omega^2 - 2\mu}{2}\right)} Q\left(\frac{\gamma_{th} + \xi_i \Omega^2 - \mu}{\Omega}\right) \tag{2.43}$$

The ergodic channel capacity of the IRS-assisted RF subsystem is given by

$$C_{RF} = \frac{1}{\ln 2} \int_0^\infty \ln(1+x) f_{\gamma_{RF}}(x) dx \tag{2.44}$$

Using [17, Eq. (2.3-31)], we can expand the modified Bessel function in (2.26) as

$$\mathrm{I}_{-\frac{1}{2}}\left(\frac{\sqrt{x\lambda}}{\delta^2}\right) = \sum_{k=0}^{\infty} \frac{\left(\frac{\sqrt{x\lambda}}{2\delta^2}\right)^{2k-0.5}}{k!\Gamma(k+0.5)} \tag{2.45}$$

Further, $\ln(1+x)$ is expressed in the form of Meijer G-function using [15, Eq.(01.04.26.0002.01)] as

$$\ln(1+x) = G_{2\ 2}^{1\ 2}\left(x \middle| \begin{matrix} 1,1 \\ 1,0 \end{matrix}\right) \tag{2.46}$$

After employing [15, Eq.(07.34.21.0088.01)], the ergodic capacity of the RF subsystem is given by

$$C_{RF} = \frac{e^{\left(\frac{-\lambda}{2\delta^2}\right)}}{\ln 2} \sum_{k=0}^{\infty} \frac{\lambda^k}{k!\,(2\delta^2)^k\,\Gamma(k+0.5)} G_{3\ 2}^{1\ 3}\left(2\delta^2 \middle| \begin{matrix} 0.5-k,1,1 \\ 1,0 \end{matrix}\right) \tag{2.47}$$

2.5 Numerical Results and Discussions

In this section, the analytical and simulations results are provided to analyze the performance of the IRS-assisted hybrid FSO/RF system. The effects of key parameters on the system performance are investigated. Further, the Monte-Carlo simulations are also presented to corroborate the proposed analysis and derived expressions. Unless otherwise stated, the parameter values assumed in our simulations are shown in Table 2.1.

Parameter	Values
FSO wavelength λ_F	1550 nm
Refractive Index Parameter C_n^2	1×10^{-13} $\mathrm{m}^{-2/3}$
Switching threshold γ_{th}	5 dB
Average SNR of RF link $\overline{\gamma}_{RF}$	-15 dB
Beam Jitter Deviation σ_θ	0.0001 rad
IRS Jitter Deviation σ_β	0.0005 rad
Link distance (Source to IRS) L_1	500 m
Link distance (IRS to Destination) L_2	500 m
Number of IRS elements for RF Transmission (N_r)	16

Table 2.1: Simulation parameters

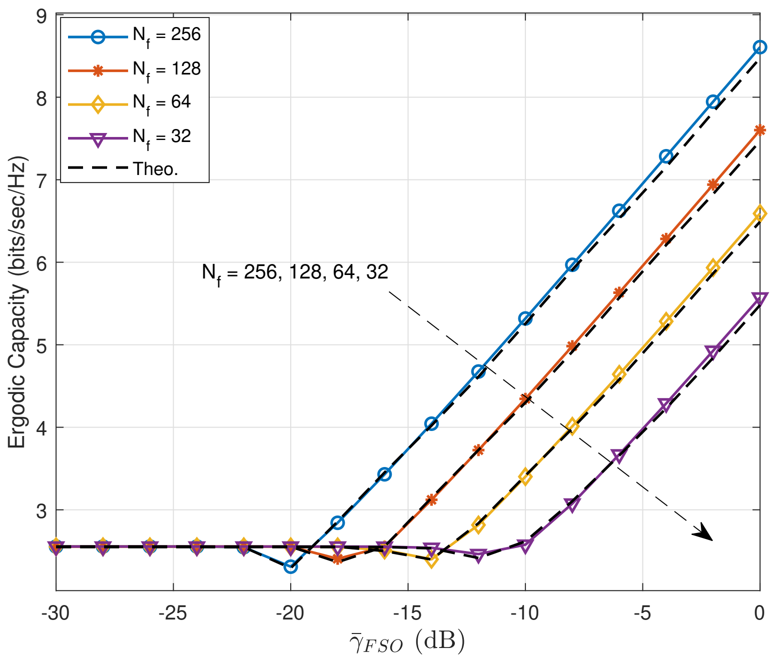

Figure 2.2: Ergodic capacity performance for different values of N_f

In Figure 2.2, the ergodic channel capacity versus average SNR of the FSO link is plotted for different number of IRS elements N_f corresponding to the FSO subsystem. It is observed that for very low average SNR values, the channel capacity is constant irrespective of the value of N_f. This is because, the hybrid system switches to the RF subsystem under very low SNR conditions with high probability and since the RF average SNR is fixed, the capacity remains constant. However, the ergodic capacity increases with increase in the average SNR of FSO link and this is due to the fact that the probability of usage of FSO subsystem will be higher compared to the RF subsystem as the average SNR increases. It is also observed that with increase in N_f, there is a significant improvement in the ergodic capacity performance with an SNR gain of around 3 dB to achieve an ergodic capacity value of 5 bits/sec/Hz.

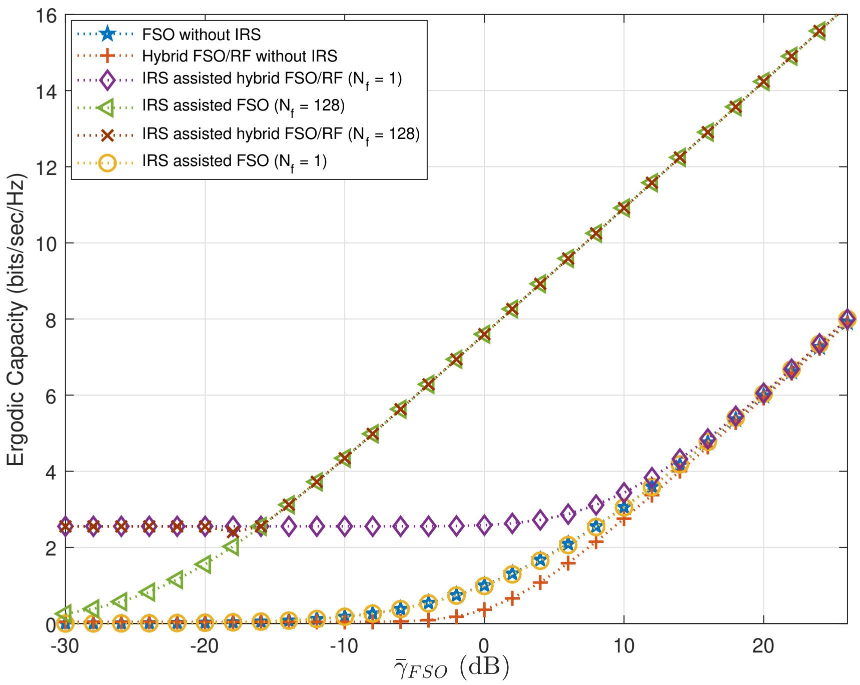

Figure 2.3: Ergodic capacity comparison for different FSO-based systems

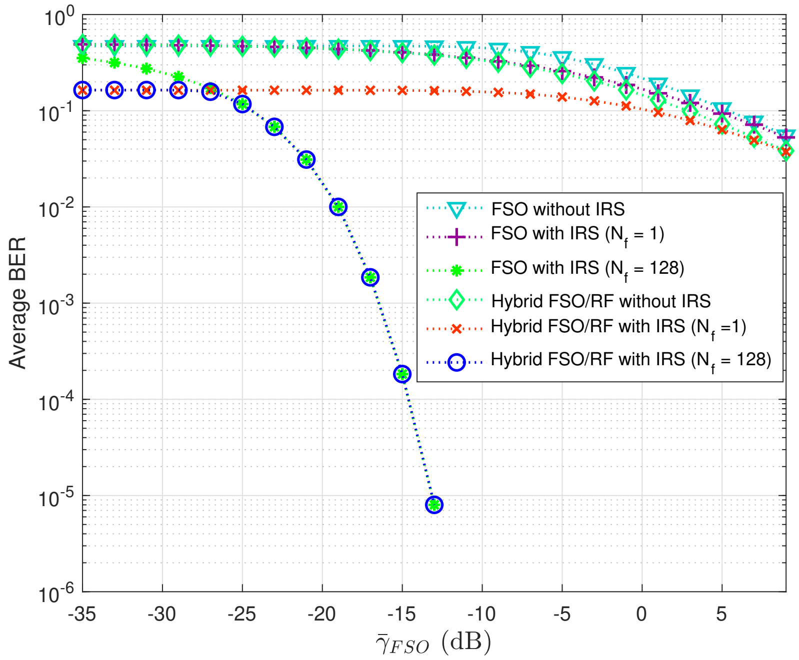

Figure 2.4: Average BER comparison for different FSO-based systems

In Figure 2.3 and Figure 2.4, the ergodic capacity and BER performances of the IRS-assisted hybrid FSO/RF system with $N_f = 1$ and 128 are compared with the FSO and hybrid FSO/RF systems without IRS and IRS-assisted FSO system with $N_f = 1$ and 128, respectively. We set average SNR of RF link as $\overline{\gamma}_{RF} = -25$ dB and switching threshold $\gamma_{th} = -3$ dB for BER performance comparison. From both the figures, it can be observed that for low average SNR values, the IRS-assisted hybrid FSO/RF system outperforms the IRS-assisted FSO system due to IRS-assisted backup RF subsystem. Meanwhile, under high-SNR conditions, both IRS-assisted FSO and hybrid FSO/RF systems achieve the same performance and outperforms the hybrid FSO/RF system without IRS. It is also interesting to note that the FSO system without IRS performs very similar to the IRS-assisted FSO system with $N_f = 1$. Hence, it is inferred that if a direct LoS path is not available between the transmitter and receiver, then IRS-assisted FSO system with $N_f = 1$ helps in creating a virtual LoS path without any deterioration in ergodic capacity and BER performances. However, it is also observed that the IRS-assisted hybrid FSO/RF system with $N_f = 1$ outperforms the hybrid FSO/RF system without IRS unlike the previous case. In case of IRS-assisted hybrid FSO/RF system, the $N_r = 16$ reflecting elements assist in improving the output SNR of RF subsystem, which in turn leads to improvement in the ergodic capacity and communication reliability compared to the hybrid FSO/RF system without IRS.

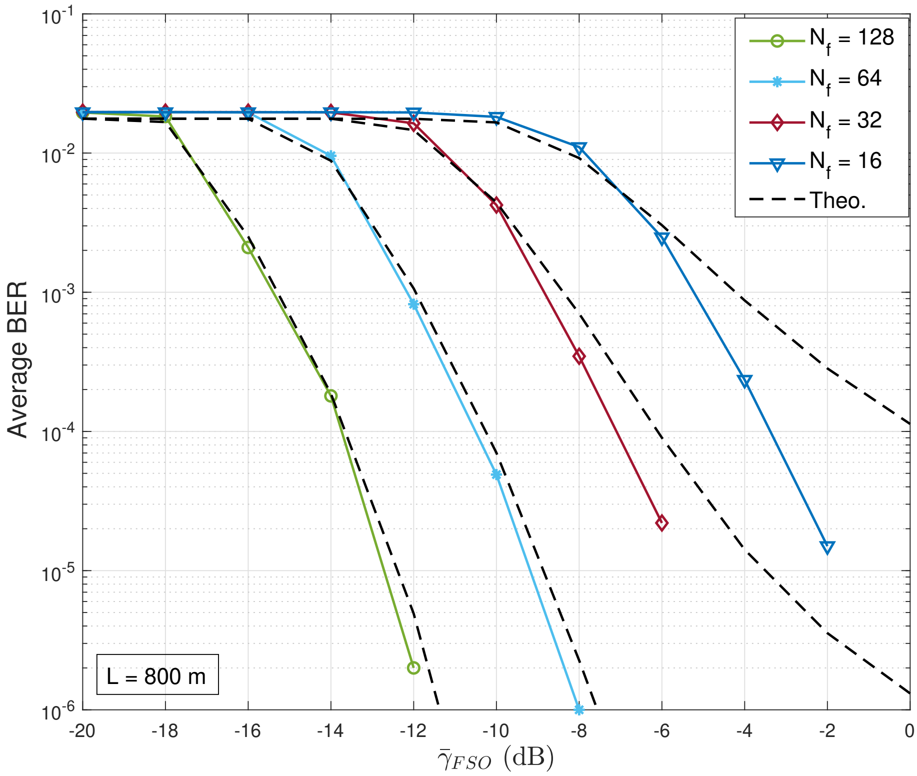

Figure 2.5: Average BER performance for different values of N_f

In Figure 2.5, the average BER versus average SNR is plotted for different values of N_f. We set $L = L_1 + L_2 = 800$ m and the other parameters are assumed as given in Table 2.1. It is observed from figure that the average BER remains constant for low average SNR values and the reason behind this trend remains the same as explained earlier in Figure 2.2. It is also to be noted that as N_f increases, the CLT approximation used to obtain the PDF of γ_{FSO} becomes tighter. This phenomenon is also evident in Figure 2.5, as the analytical BER curves for $N_f = 128$ and $N_f = 64$ almost well agree with the simulation curves compared to the performance curves with $N_f = 16$ and $N_f = 32$. Furthermore, it is also noticed that doubling N_f gives approximately 3 to 5 dB improvement in the required SNR to achieve the target BER of 10^{-3}.

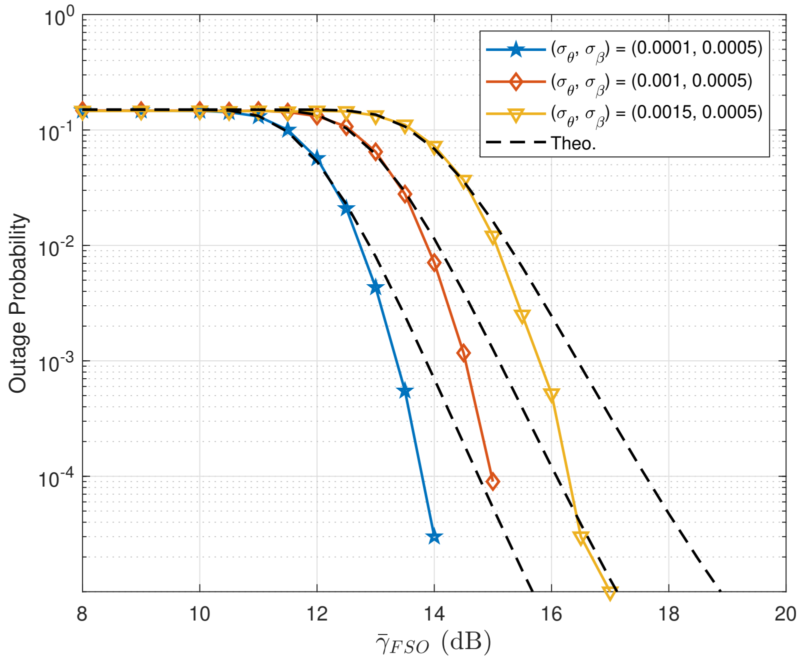

Figure 2.6: Outage performance for different beam jitter deviation values

Figure 2.6 shows the outage performance versus average SNR for different values of beam jitter deviation σ_θ. We set $L = 300$ m, $\alpha = 11$, $\beta = 9$, and $N_f = 128$. Here, when the values of IRS jitter and beam jitter deviation increases, the outage performance of the hybrid FSO/RF system deteriorates. This is because, the pointing error severity increases with increasing value of jitter deviation. Further, the deviation of analytical outage curves from the simulation curves in Figure 2.6, especially in the high-SNR region, is mainly due to the CLT approximation, which is not very tight for low values of N_f.

2.6 Conclusions

In this chapter, a comprehensive performance analysis of the IRS-assisted hybrid FSO/RF system was carried out and the closed-form expressions for the outage probability, average BER, and ergodic capacity were derived assuming single-threshold-based switching scheme. The atmospheric turbulence of each FSO link in the cascaded channels was modeled using Gamma-Gamma distribution and small-scale fading of each RF link in the cascaded RF channels was assumed to follow Rayleigh distribution. In addition, the pointing errors due to beam jitter and IRS jitter was also taken into consideration in our analysis. From the numerical results, it was inferred that the performance improvement is obtained with increase in the number of IRS elements of FSO link N_f as well as the analytical results well agree with the simulation results for the case when N_f is high. It was also mainly observed that the performance of the IRS-assisted hybrid FSO/RF system is better in terms of both average BER and ergodic capacity compared to the IRS-assisted FSO system as well as FSO and hybrid FSO/RF systems without IRS.

Chapter 3

Performance Analysis of IRS-Assisted Mixed FSO/RF Communication System

3.1 Introduction

The closed-form expressions of performance metrics for the IRS-assisted hybrid FSO/RF communication system model are derived in Chapter 2 considering Gamma-Gamma fading channel for FSO subsystem and Rayleigh fading channel for RF subsystem. It is also shown in Chapter 2 that the aid of IRS has significantly improved the system performance of hybrid FSO/RF system. Another such system where IRS can be of great assistance to improve system coverage and signal quality is mixed FSO/RF system. This chapter describes an IRS-assisted mixed FSO/RF system model. In the proposed system model, we considered a FSO link and a RF link cascaded using a decode-and-forward (DF) relaying protocol to convert optical signal to RF signal. It is assumed that there is no direct link between source (S), relay (R), and destination (D), hence both links are assisted with IRS. Further, transmitters and receivers at S, R, and D are considered to be single aperture or antenna devices. The performance of this proposed system is analyzed by obtaining the closed-form expressions of outage probability and average BER.

3.2 Organisation of Chapter

The rest of the chapter is organized as follows: The system model for IRS-assisted mixed FSO/RF system has been discussed in Section 3.3 and Section 3.4 provides the closed-form expressions for the outage probability and ergodic capacity over Malaga fading channel for FSO subsystem and Rayleigh fading channel for RF subsystem. Furthermore, numerical results and inferences are given in Section 3.5. Finally, the concluding remarks are given in Section 3.6.

3.3 System Model

We consider an IRS-assisted mixed FSO/RF system as shown in Figure 3.1. The system consists of an optical source with single aperture, a relay with both FSO and RF capability and a destination with RF receiver. Due to the assumption that there is no direct LoS between either S, R, and D, we have employed two IRS, i.e. between S and R as well as between R and D. The message signal is first being transmitted from S to R via FSO link with the help of the IRS. The FSO signal is detected either by heterodyne detection (HD) or index modulation/direct detection (IM/DD) technique. After that, the optical signal is decoded at R and re-transmitted to D via RF link also with the help of IRS. It is further assumed that CSI is perfectly available at the receivers of both FSO and RF subsystems.

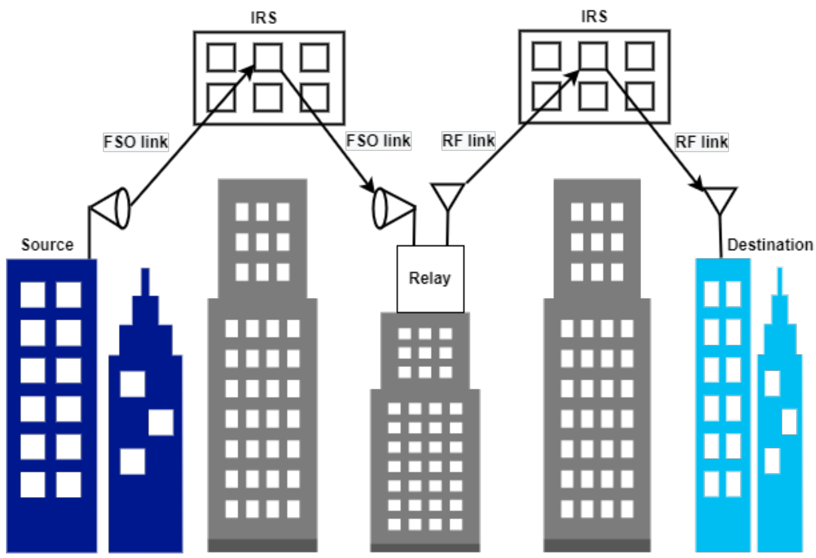

Figure 3.1: System model for IRS-assisted mixed FSO/RF communication system

3.3.1 FSO Channel Model

For FSO subsystem, we have considered a sub-carrier intensity modulation (SIM) with binary phase-shift-keying (BPSK) scheme at the transmitter. At the receiver, both HD detection and IM/DD detection techniques have been assumed to detect FSO signals. There is a single FSO link between transmitter and receiver via IRS. In Chapter 2, we considered Gamma-Gamma fading to model atmosphere turbulence, but in this chapter we have assumed a more generalized fading distribution, i.e. Malaga distribution to model the atmospheric turbulence. The main signal impairments are atmospheric turbulence h_a and pointing errors h_p.

Atmospheric Turbulence Model:

The end-to-end atmospheric turbulence is the cascaded turbulence from S to IRS and from IRS to R given as

$$h_a = h_{a_1} h_{a_2} \tag{3.1}$$

where h_{a_1} and h_{a_2} denote the atmospheric turbulence-induced fading coefficients from FSO transmitter to IRS and IRS to FSO receiver, respectively. Let L_1 and L_2 denote the distances between the transmitter and IRS and the IRS and receiver, respectively. Further, we assume IRS is placed at the middle of transmitter and receiver such that $L_1 = L_2 = L$. The Gamma-Gamma distribution is used to model only moderate-to-strong turbulence levels and hence, we have used a more generalised distribution, i.e. Malaga distribution to model the turbulence of the FSO link. Its PDF is given by [22, Eq. (24)]

$$f_{h_{a_i}}(x) = A \sum_{m_i=1}^{\beta} a_{m_i} x^{\left(\frac{\alpha+m_i}{2}-1\right)} \mathrm{K}_{\alpha-m_i}\left(2\sqrt{\frac{\alpha\beta}{g\beta+\Omega'}}\right) \qquad i \in \{1,2\} \tag{3.2}$$

The PDF of end-to-end atmospheric turbulence can be derived by solving the integral given by

$$f_{h_a}(x) = \int_0^\infty f_{h_{a_1}}(t) f_{h_{a_2}}\left(\frac{x}{t}\right) \frac{1}{t} dt \tag{3.3}$$

After substituting (3.2) in (3.3) and simplifying, we get

$$f_{h_a}(x) = A^2 \sum_{m_1=1}^{\beta} \sum_{m_2=1}^{\beta} a_{m_1} a_{m_2} x^{\left(\frac{\alpha+m_2}{2}-1\right)} \int_0^\infty t^{\left(\frac{m_1-m_2}{2}-1\right)} \mathrm{K}_{\alpha-m_1}\left(2\sqrt{P}\right) \mathrm{K}_{\alpha-m_2}\left(2\sqrt{P}\right) dt \tag{3.4}$$

where $P = \left(\frac{\alpha\beta}{g\beta+\Omega'}\right)$. We can write the modified Bessel function of second kind in the form Meijer-G function [15, Eq. (03.04.26.0008.01)] and solving the integral using [15, Eq. (07.34.17.0012.01)] and [15, Eq. (07.34.21.0011.01)] to obtain the PDF of end-to-end atmospheric turbulence as

$$f_{h_a}(x) = A^2 \sum_{m_1=1}^{\beta} \sum_{m_2=1}^{\beta} a_{m_1} a_{m_2} x^{\left(\frac{\alpha+m_2}{2}-1\right)} P^{\left(\frac{m_1-m_2}{2}\right)} \times G_{0\,4}^{4\,0}\left(P^2 x \middle| \begin{matrix} - \\ \frac{\alpha-m_2}{2}, \frac{m_2-\alpha}{2}, \frac{\alpha-m_2}{2}, m_1-\left(\frac{\alpha+m_2}{2}\right) \end{matrix}\right) \tag{3.5}$$

Pointing Error Model:

As discussed in section 2.3.1, the end-to-end pointing errors due to beam and IRS jitter is given by [8]

$$h_p \approx A_0 \exp\left(-\frac{2r^2}{w_{zeq}}\right) \tag{3.6}$$

where r is the radial displacement caused by beam and IRS jitter, A_0 represents the fraction of power at the receiver aperture, and w_{zeq} is the equivalent beam width. The PDF of the end-to-end pointing error is given by

$$f_{h_p}(x) = \frac{c}{A_0}\left(\frac{x}{A_0}\right)^{c-1}, 0 < x < A_0 \tag{3.7}$$

where c is the pointing error coefficient. For more detailed description, see section 2.3.1.

Combined Channel Model:

The combined channel irradiance for the k^{th} link is the product of atmospheric turbulence and pointing errors, and is given by

$$h_{fso} = h_a h_p \tag{3.8}$$

The PDF of the combined channel irradiance is obtained by solving the integral

$$f_{h_{fso}}(x) = \int_{\frac{x}{A_0}}^{\infty} f_{h_a}(t) f_{h_p}\left(\frac{x}{t}\right)\frac{1}{t}dt \tag{3.9}$$

After substituting (3.5) and (3.7) in (3.9) and simplifying, we obtain

$$f_{h_{fso}}(x) = \frac{A^2 c}{4} \sum_{m_1=1}^{\beta} \sum_{m_2=1}^{\beta} a_{m_1} a_{m_2} P^{\left(\frac{m_1-m_2}{2}\right)} \left(\frac{x}{A_0}\right)^{\frac{\alpha+m_2}{2}} x^{-1} \times G_{0\,4}^{4\,0}\left(P^2\left(\frac{x}{A_0}\right) \middle| \begin{matrix} 1+c-\frac{\alpha+m_2}{2} \\ c-\frac{\alpha+m_2}{2}, \frac{\alpha-m_2}{2}, \frac{m_2-\alpha}{2}, \frac{\alpha-m_2}{2}, m_1-\left(\frac{\alpha+m_2}{2}\right) \end{matrix}\right) \tag{3.10}$$

We can further simplify this equation by using [15, Eq. 07.34.17.0011.01] as

$$f_{h_{fso}}(x) = \frac{A^2 c}{4} \sum_{m_1=1}^{\beta} \sum_{m_2=1}^{\beta} a_{m_1} a_{m_2} P^{-\left(\alpha + \frac{m_1+m_2}{2}\right)} x^{-1} G_{1\,5}^{5\,0}\left(P^2 \left(\frac{x}{A_0}\right) \middle| \begin{matrix} 1+c \\ c, \alpha, m_2, \alpha, m_1 \end{matrix} \right) \tag{3.11}$$

Also, we can derive the expected value of h_{fso} as

$$E[h_{fso}] = E[h_a h_p] \tag{3.12}$$

Since, h_a and h_p are independent, thus we can write $E[h_{fso}]$ as

$$E[h_{fso}] = E[h_a]E[h_p] \tag{3.13}$$

Further, $h_a = h_{a_1} h_{a_2}$ and both h_{a_1} and h_{a_2} are also independent to each other hence, $E[h_{fso}]$ becomes

$$E[h_{fso}] = E[h_{a_1}]E[h_{a_2}]E[h_p] \tag{3.14}$$

From [22, Eq. (27)], the expected value of $E[h_{a_1}]$ and $E[h_{a_2}]$ after simplification is calculated as

$$E[h_{a_1}] = E[h_{a_2}] = (\Omega' + g) \tag{3.15}$$

We can calculate $E[h_p]$ by solving the integral

$$\begin{aligned} E[h_p] &= \int_0^{\infty} x f_{h_p}(x) dx = \int_0^{\infty} c \left(\frac{x}{A_0}\right)^c dx \qquad 0 < x < A_0 \\ &= \int_0^{A_0} c \left(\frac{x}{A_0}\right)^c dx = c \left[\frac{x^{(c+1)}}{(c+1)A_0^c} \right]_0^{A_0} \\ &= \frac{cA_0}{c+1} \end{aligned} \tag{3.16}$$

Substituting (3.15) and (3.16) in (3.14), we obtain $E[h_{fso}]$ as

$$E[h_{fso}] = (\Omega' + g)^2 \frac{cA_0}{c+1} \tag{3.17}$$

Instantaneous SNR:

The instantaneous SNR of the FSO link γ_{FSO} is given by

$$\gamma_{FSO} = \frac{(P_F \eta h_{fso})^a}{\sigma_0^2} \tag{3.18}$$

where P_F is transmitted optical power, η is the receiver's optical to electrical efficiency, σ_0^2 is the additive white Gaussian noise (AWGN) variance, and a is the parameter that describes the detection technique used (i.e. $a = 1$ means HD detection technique and $a = 2$ means IM/DD detection technique). Additionally, the average electrical SNR is obtained as

$$\overline{\gamma}_{FSO} = \frac{(P_F\eta)^a}{\sigma_0^2}(E[h_{fso}])^a \tag{3.19}$$

Substituting (3.17) in (3.19), we get

$$\overline{\gamma}_{FSO} = \frac{(P_F\eta)^a}{\sigma_0^2}\left[(\Omega'+g)^2\frac{cA_0}{c+1}\right]^a = \frac{(P_F\eta)^a}{\sigma_0^2}M_1^a \tag{3.20}$$

where $M_1 = (\Omega'+g)^2\frac{cA_0}{c+1}$. By substituting value of σ_0^2 from (3.20) in (3.18), the instantaneous SNR can be written in the form of average electrical SNR as

$$\gamma_{FSO} = \frac{\overline{\gamma}_{FSO}h_{fso}^a}{M_1^a} \tag{3.21}$$

Using the power transformation of the random variable, the PDF of γ_{FSO} can obtained as

$$f_{\gamma_{FSO}}(x) = \frac{A^2c}{4a}\sum_{m_1=1}^{\beta}\sum_{m_2=1}^{\beta}a_{m_1}a_{m_2}P^{-\left(\alpha+\frac{m_1+m_2}{2}\right)}x^{-1}G_{1\,5}^{5\,0}\left(\frac{P^2M_1}{A_0}\left(\frac{x}{\overline{\gamma}_{FSO}}\right)^{\frac{1}{a}}\middle|\begin{matrix}1+c\\ c,\alpha,m_2,\alpha,m_1\end{matrix}\right) \tag{3.22}$$

Further, the CDF of γ_{FSO} is obtained by using [15, Eq. (07.34.21.0084.01)] as

$$\begin{aligned}F_{\gamma_{FSO}}(x) = &\frac{A^2c}{4a(2\pi)^{2(a-1)}}\sum_{m_1=1}^{\beta}\sum_{m_2=1}^{\beta}a_{m_1}a_{m_2}P^{-\left(\alpha+\frac{m_1+m_2}{2}\right)}a^{(2\alpha+m_1+m_2-2)}\\ &\times G_{a+1\;5a+1}^{5a\;\;1}\left(\left(\frac{P^2M_1}{A_0}\right)^a\frac{x}{a^{4a}\overline{\gamma}_{FSO}}\middle|\begin{matrix}1,\Delta_1\\ \Delta_2,0\end{matrix}\right)\end{aligned} \tag{3.23}$$

where $\Delta_1 = \frac{c+1}{a},\ldots,\frac{c+a}{a}$ and $\Delta_2 = \frac{c}{a},\ldots,\frac{c+a-1}{a},\frac{\alpha}{a},\ldots,\frac{\alpha+a-1}{a},\frac{m_2}{a},\ldots,\frac{m_2+a-1}{a},\frac{\alpha}{a},\ldots,\frac{\alpha+a-1}{a},\frac{m_1}{a},\ldots,\frac{m_1+a-1}{a}$.

3.3.2 RF Channel Model

The RF channel is modeled by assuming Rayleigh fading. The channel model is discussed in detail inside section 2.3.2.

3.4 Performance Analysis

3.4.1 Outage Probability

The IRS-assisted mixed FSO/RF system will go into outage when FSO or RF subsystem goes into outage, i.e. if the instantaneous SNR of either FSO subsystem γ_{FSO}, or RF subsystem γ_{RF}, falls below a certain threshold SNR γ_{th}. Thus, the outage probability of the system is given as

$$\begin{aligned}
P_{out} &= \Pr(\gamma_{FSO} < \gamma_{th} \text{ or } \gamma_{RF} < \gamma_{th}) = 1 - \Pr(\gamma_{FSO} > \gamma_{th} \text{ and } \gamma_{RF} > \gamma_{th}) \\
&= 1 - \left[\left(1 - F_{\gamma_{FSO}}(\gamma_{th})\right)\left(1 - F_{\gamma_{RF}}(\gamma_{th})\right)\right] \\
&= F_{\gamma_{FSO}}(\gamma_{th}) + F_{\gamma_{RF}}(\gamma_{th}) - F_{\gamma_{FSO}}(\gamma_{th}) F_{\gamma_{RF}}(\gamma_{th}) \qquad (3.24)
\end{aligned}$$

The expressions for $F_{\gamma_{FSO}}(\gamma_{th})$ and $F_{\gamma_{RF}}(\gamma_{th})$ are given by (3.23) and (2.27), respectively.

3.4.2 Average BER

In this section, we analyze the average BER of the IRS-assisted mixed FSO/RF system. Let P_{e1} is the BER generated in the FSO link and P_{e2} is the BER generated in the RF link. From [23, Eq. (14)], the average BER for the IRS-assisted mixed FSO/RF system P_e^M assuming BPSK signalling is given by

$$P_e^M = P_{e1} + P_{e2} - 2P_{e1}P_{e2} \qquad (3.25)$$

The average BER of IRS-assisted FSO subsystem is calculated by solving the integral below

$$P_{e1} = \int_0^\infty \frac{1}{2} \operatorname{erfc}(\sqrt{\gamma}) f_{\gamma_{FSO}}(\gamma) d\gamma, \qquad (3.26)$$

The complimentary error function can be written in the form of Meijer-G function from [15, Eq. (06.27.26.0006.01)] as

$$\operatorname{erfc}(\sqrt{z}) = \frac{1}{\sqrt{\pi}} G_{1\,2}^{2\,0}\left(z \middle| \begin{matrix} 1 \\ 0, \frac{1}{2} \end{matrix} \right) \qquad (3.27)$$

Substituting (3.27) and (3.22) in (3.26) and simplifying, we get

$$\begin{aligned}
P_{e1} &= \frac{A^2 c}{8a\sqrt{\pi}} \sum_{m_1=1}^{\beta} \sum_{m_2=1}^{\beta} a_{m_1} a_{m_2} P^{-\left(\alpha + \frac{m_1+m_2}{2}\right)} \\
&\times \int_0^\infty \gamma^{-1} G_{1\,2}^{2\,0}\left(\gamma \middle| \begin{matrix} 1 \\ 0, \frac{1}{2} \end{matrix} \right) G_{1\,5}^{5\,0}\left(\frac{P^2 M_1}{A_0} \left(\frac{\gamma}{\overline{\gamma}_{FSO}} \right)^{\frac{1}{a}} \middle| \begin{matrix} 1+c \\ c, \alpha, m_2, \alpha, m_1 \end{matrix} \right) d\gamma \qquad (3.28)
\end{aligned}$$

Solving the integral using [15, Eq. (07.34.21.0013)], P_{e1} is given as

$$\begin{aligned}
P_{e1} &= \frac{A^2 c}{8a\sqrt{\pi}(2\pi)^{2(a-1)}} \sum_{m_1=1}^{\beta} \sum_{m_2=1}^{\beta} a_{m_1} a_{m_2} P^{-\left(\alpha + \frac{m_1+m_2}{2}\right)} a^{(2\alpha + m_1 + m_2 - 2)} \\
&\times G_{a+2\;5a+1}^{5a\;\;\;2}\left(\left(\frac{P^2 M_1}{A_0} \right)^a \frac{a^{-4a}}{\overline{\gamma}_{FSO}} \middle| \begin{matrix} 1, \frac{1}{2}, \Delta_1 \\ \Delta_2, 0 \end{matrix} \right) \qquad (3.29)
\end{aligned}$$

The average BER of IRS-assisted RF subsystem P_{e2} is given by (2.37) and (2.38) in section 2.4.2.

3.5 Numerical Results and Discussions

In this section, we will analyze the derived closed-form expressions. We also observed the effects of key parameters on outage probability and average BER of the system. Monte-Carlo simulations are also presented to corroborate the proposed analysis and derived expressions. Unless otherwise stated, the parameter values assumed in our simulations are shown in Table 3.1.

Parameter	**Values**
FSO wavelength λ_F	1550 nm
Refractive Index Parameter C_n^2	5×10^{-15} m$^{-2/3}$
Switching threshold γ_{th}	5 dB
Effective number of large-scale cells α	7.3
Amount of fading parameter β	7
Pointing error coefficient c	1.27
Link distance (Source to IRS) L_1	3000 m
Link distance (IRS to Destination) L_2	3000 m
Number of IRS elements for RF Transmission N_r	32

Table 3.1: Simulation parameters

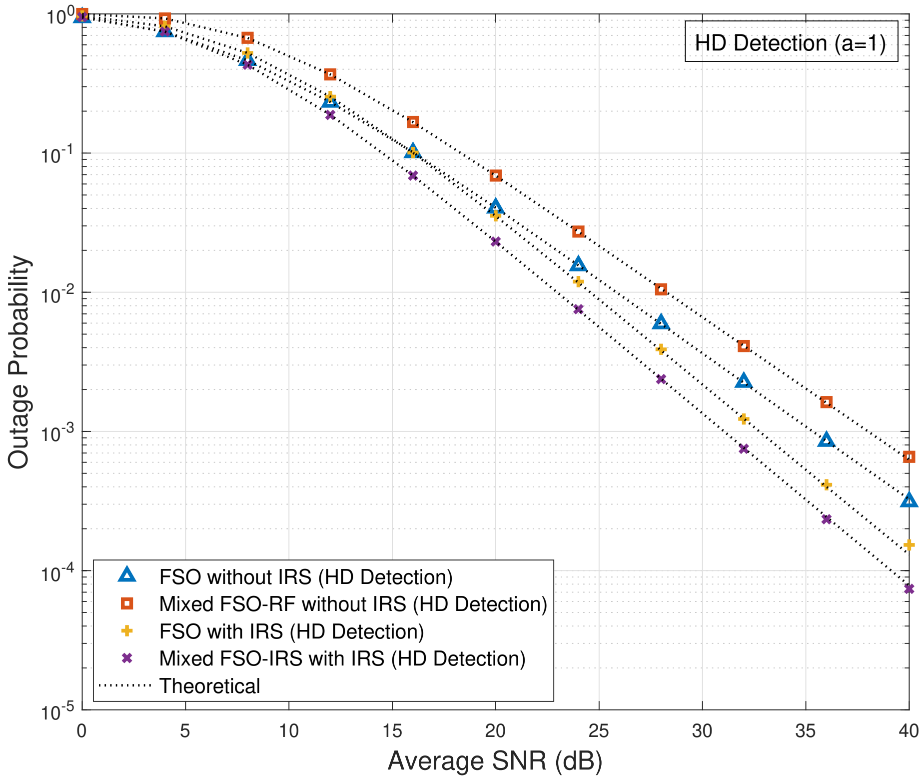

Figure 3.2: Outage probability comparison for different FSO-based systems

Figure 3.2 shows outage probability versus average SNR plot for different FSO-based system for HD technique. To achieve the outage probability of 10^{-3}, the average SNR required for FSO system without IRS, mixed FSO/RF system without IRS, IRS-assisted FSO system, and IRS-assisted mixed FSO/RF system are 35.5 dB, 38 dB, 33 db, and 31 dB, respectively. Moreover, SNR gains achieved by the IRS-assisted mixed FSO/RF system with respect to FSO system without IRS, mixed FSO/RF system without IRS, and IRS-assisted FSO system are 4.5 dB, 7 dB and 2 dB, respectively. From this we infer that IRS-assisted FSO/RF system performs better than each of the compared system in terms of outage probability. Note that a significant SNR gain of approximately 7 dB is achieved using the IRS-assisted mixed FSO/RF system over mixed FSO/RF system without IRS for outage probability of 10^{-3}. This improvement is beacause in IRS-assisted mixed FSO/RF system, the instantaneous SNR at the RF link is maximised by cancelling out the phases from each multi-path signal with the help of IRS.

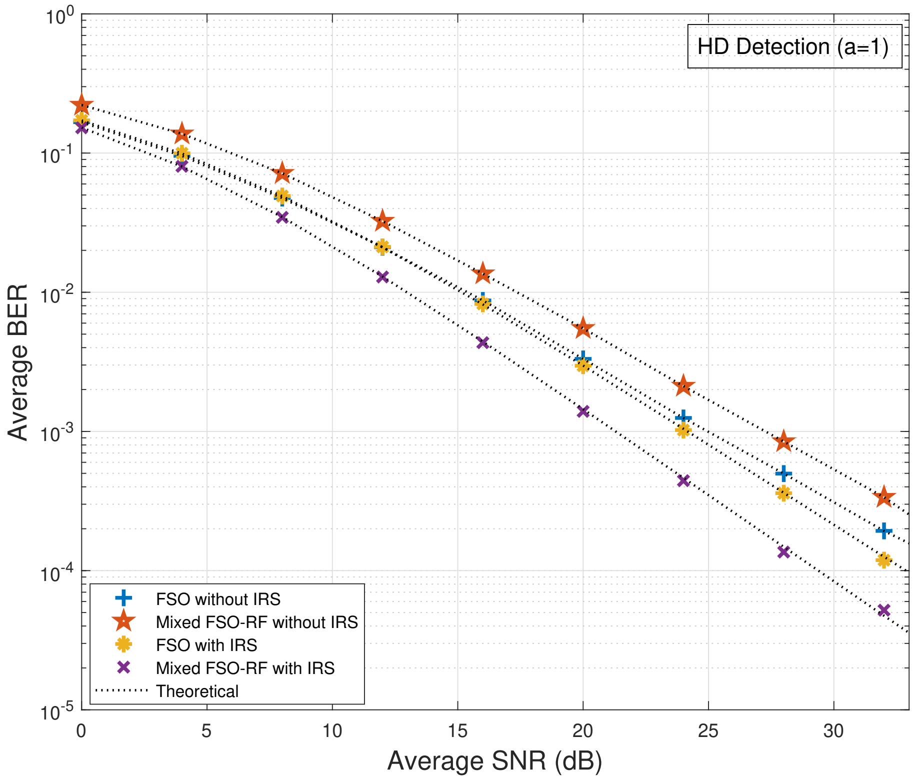

Figure 3.3: Average BER comparison for different FSO-based systems

In Figure 3.3, average BER versus average SNR plot for different FSO-based system for HD detection technique is plotted. To achieve the average BER of 10^{-3}, the average SNR required for FSO system without IRS, mixed FSO/RF system without IRS, IRS-assisted FSO system, and IRS-assisted mixed FSO/RF system are 25 dB, 27.5 dB, 24.5 db, and 21 dB, respectively. In addition, the SNR gains achieved by IRS-assisted mixed FSO/RF system with respect to FSO system without IRS, mixed FSO/RF system without IRS, and IRS-assisted FSO system are 4 dB, 6.5 dB and 3.5 dB, respectively. Therefore, it is inferred that IRS-assisted FSO/RF system performs better than each of the compared system in terms of average BER. Further, The significant SNR gain of 6.5 dB for 10^{-3} average BER by using IRS-assisted mixed FSO/RF system over mixed FSO/RF system without IRS is mainly contributed by the maximisation of SNR at the RF link from using IRS.

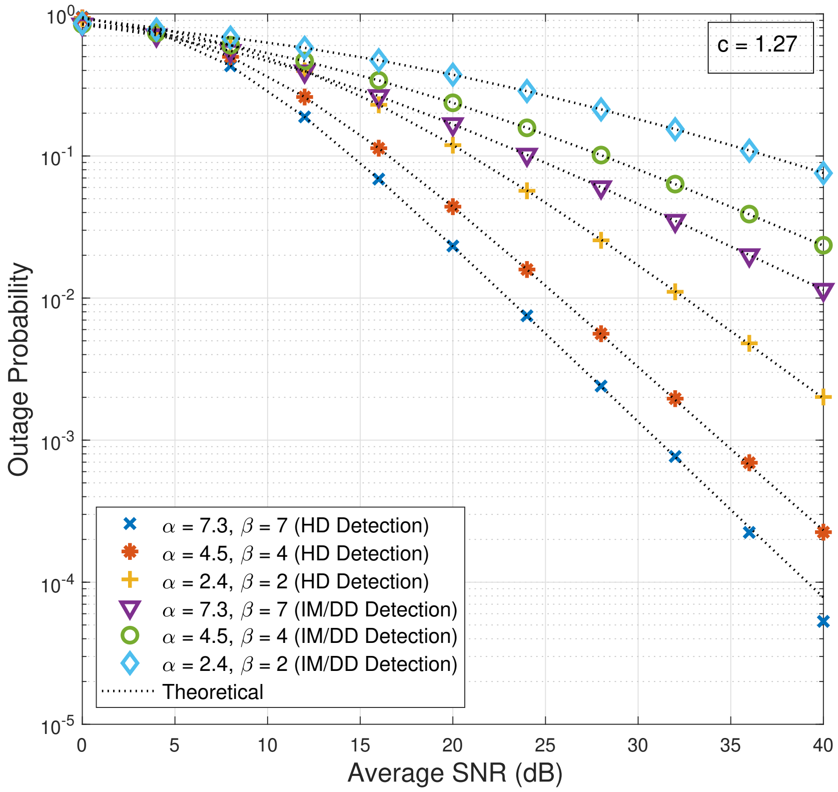

Figure 3.4: Outage performance for different atmospheric turbulence levels

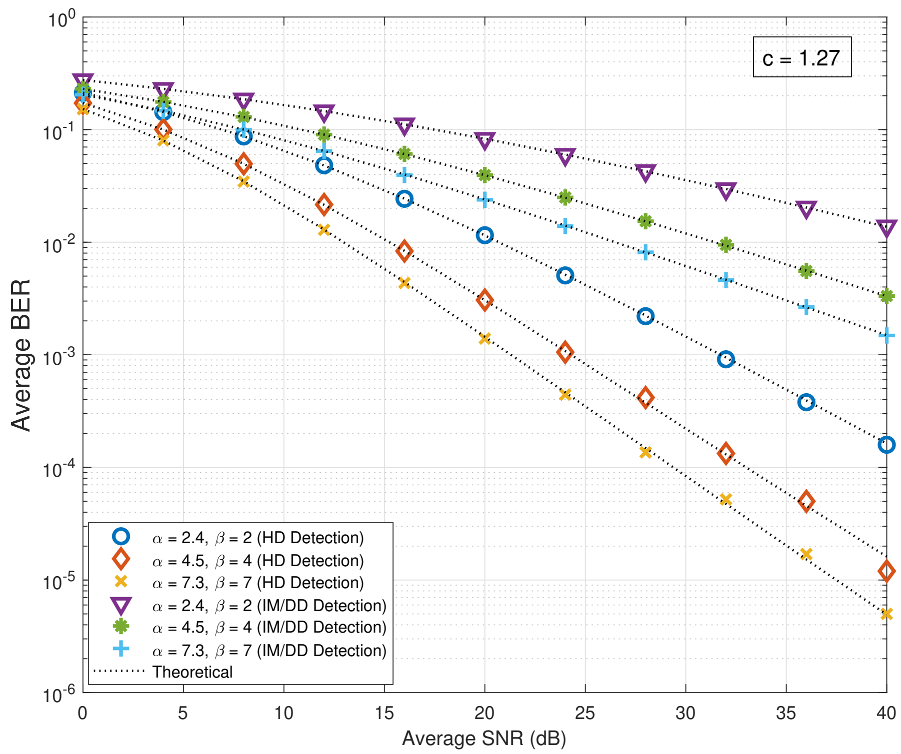

Figure 3.5: Average BER performance for different atmospheric turbulence levels

Figure 3.4 and Figure 3.5 show the effect of atmospheric turbulence levels on outage probability and average BER of the IRS-assisted mixed FSO/RF system. From each figure, we can observe that if the value of parameters, α and β decreases (i.e. turbulence increases), the performance of the system deteriorates in terms of both outage probability and average BER. It can be also inferred from the figures that in each case, HD technique outperforms IM/DD technique due to coherent detection nature of HD technique.

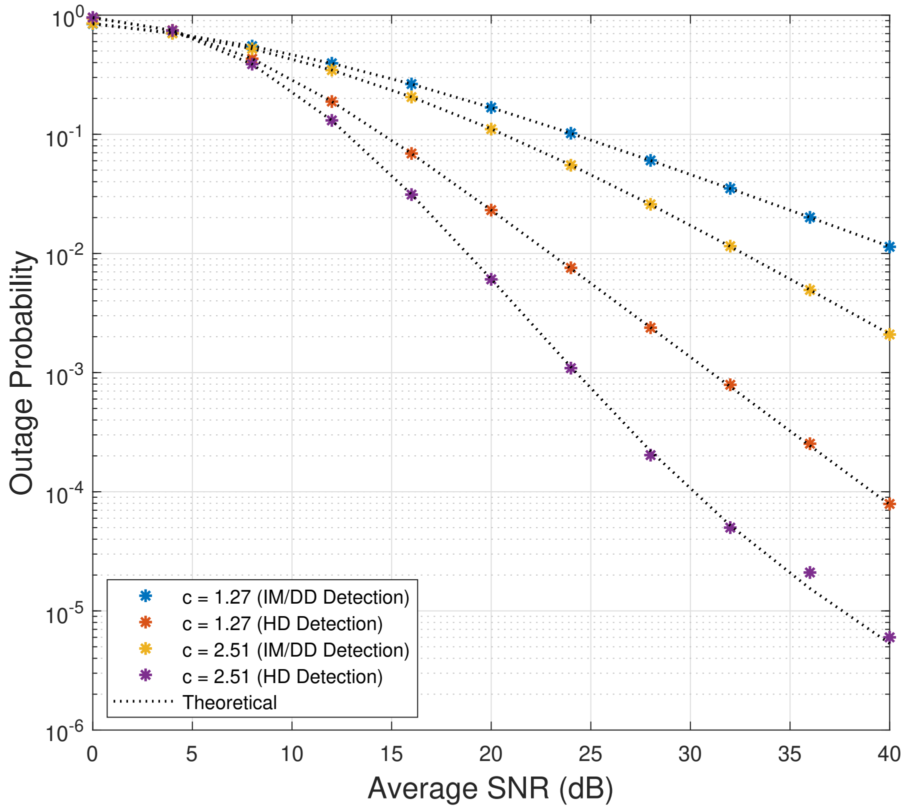

Figure 3.6: Outage performance for different pointing errors

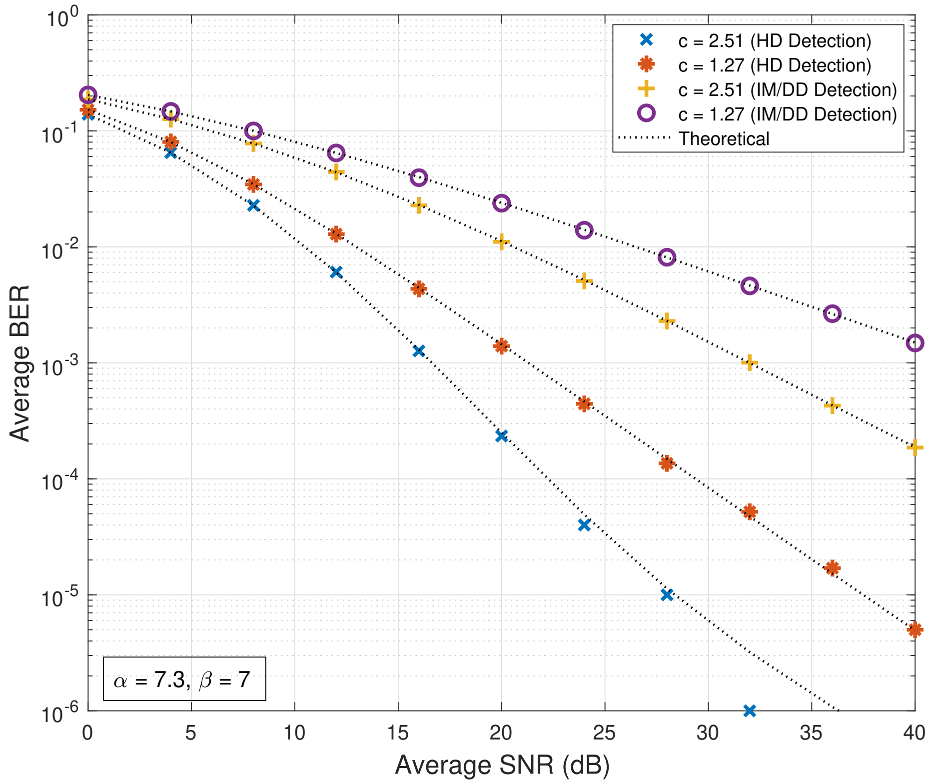

Figure 3.7: Average BER performance for different pointing errors

Figure 3.6 and Figure 3.7 show the effect of pointing errors on outage probability and average BER of the IRS-assisted mixed FSO/RF system. From both figures, we observe that the performance of the system is worse in terms of outage probability and average BER for pointing error coefficient c value 1.27 (i.e. strong pointing error) compared to pointing error coefficient c value 2.51 (i.e. moderate pointing error). Furthermore, it can be noticed from the figures that in each case, HD detection technique is better than IM/DD detection technique. This should also be noted that for every plot, as the average SNR increases, the system performance improves. This is due to the increase in strength of signal with respect to noise.

3.6 Conclusions

In this chapter, the performance analysis of the IRS-assisted mixed FSO/RF communication system model is done by deriving the closed-form expressions for outage probability and average BER. The generalized Malaga distribution is considered for characterizing the FSO fading channel and Rayleigh distribution is considered for modeling the RF fading channel. Furthermore, the derived closed-form expression of outage probability and average BER for the proposed model are implemented in MATLAB and Monte-Carlo simulations are performed to verify the derived expressions. From simulation results, it is observed that the IRS-assisted mixed FSO/RF system performs better than every other FSO-based system and in consideration with a significant SNR gain from mixed FSO/RF system without IRS in terms of both outage probability and average BER. The system performance for different key parameters namely, atmospheric turbulence (α, β) and pointing errors (c) is analyzed. It is seen that if the turbulence levels and pointing errors become worse, then the outage probability of the system increases. Similar trends can be seen for average BER performance. Hence, the system performance deteriorates with increase in atmospheric turbulence and pointing errors. The performance of the system for different detection technique used at FSO receiver has also been studied and it is inferred that HD technique gives much better results than IM/DD technique.

Chapter 4

Conclusions and Future Works

This thesis examines the performance of the following two system models: IRS-assisted hybrid FSO/RF communication system and IRS-assisted mixed FSO/RF communication system. In IRS-assisted hybrid FSO/RF system, the analytical framework has been carried out over Gamma-Gamma fading channel for FSO subsystem and Rayleigh fading channel for RF subsystem, whereas, in case of IRS-assisted mixed FSO/RF system, the analytical framework has been carried out over Malaga fading channel for FSO subsystem and Rayleigh fading channel for RF subsystem. The derived closed-form expressions for performance metrics are validated by Monte-Carlo simulations.

4.1 Conclusions

In Chapter 2, we investigated the performance of the proposed system model of IRS-assisted hybrid FSO/RF communication system based on the hard-switching scheme. The closed-form expressions for performance metrics such as outage probability, average BER, and ergodic channel capacity are derived and implemented in MATLAB. Numerical results explained the effect of the number of FSO links on average BER and ergodic channel capacity of the proposed system. Additionally, we observe the effects of pointing errors on outage probability of our system. Our proposed system model is better in terms of both average BER and ergodic capacity compared to the IRS-assisted FSO system as well as FSO and hybrid FSO/RF systems without IRS.

In Chapter 3, we have investigated the IRS-assisted mixed FSO/RF communication system model. The closed-form expressions for performance metrics such as outage probability and average BER of the proposed system model are derived and implemented in MATLAB. From the numerical results, we have observed the effect of pointing errors and atmospheric turbulence on the system. We also compared proposed system model with other FSO-based systems in the literature. Our proposed model is better in terms of outage probability and average BER compared to IRS-assisted FSO as well as FSO and mixed FSO/RF systems without IRS.

4.2 Future Works

The scope for the future work can be summarized as follows

- The performance of IRS-assisted hybrid FSO/RF and mixed FSO/RF system have been carried considering Rayleigh fading model for RF channel. However, a more generalized fading channel can be considered.
- The performance analysis of IRS-assisted mixed FSO/RF system was done for single link FSO subsystem. Further analysis can be carried out for multiple link FSO subsystem.
- The IRS-assisted hybrid FSO/RF system was analyzed based on hard-switching scheme. However, much better results can be obtained by considering adaptive combining technique.
- In both of our proposed models, we have assumed that there is no LoS between the transmitter and receiver. But we can still use IRS even if there is a direct LoS between the transmitter and receiver. The performance of the system assuming the presence of direct LoS can be analyzed.
- In our work, we have not investigated the performance of the system in terms of asymptotic analysis which is calculated at the high SNR conditions. The same can be explored in our future work.

Publications from Thesis

1. Sandesh Sharma, Naredra Vishwakarma, and Swaminathan R, “Performance analysis of IRS-assisted hybrid FSO/RF communication system,” in proceedings of *2022 IEEE National Conference on Communications (NCC)*, pp. 1-6.

Bibliography

[1] Marco Di Renzo et al. “Smart Radio Environments Empowered by Reconfigurable Intelligent Surfaces: How It Works, State of Research, and The Road Ahead”. In: *IEEE Journal on Selected Areas in Communications* 38.11 (2020), pp. 2450–2525. DOI: 10.1109/JSAC.2020.3007211.

[2] Wankai Tang et al. “Wireless Communications With Reconfigurable Intelligent Surface: Path Loss Modeling and Experimental Measurement”. In: *Trans. Wireless. Comm.* 20.1 (Jan. 2021), pp. 421–439. ISSN: 1536-1276. DOI: 10.1109/TWC.2020.3024887. URL: https://doi.org/10.1109/TWC.2020.3024887.

[3] Ertugrul Basar et al. “Wireless Communications Through Reconfigurable Intelligent Surfaces”. In: *IEEE Access* 7 (2019), pp. 116753–116773. DOI: 10.1109/ACCESS.2019.2935192.

[4] Mostafa Zaman Chowdhury et al. “6G Wireless Communication Systems: Applications, Requirements, Technologies, Challenges, and Research Directions”. In: *IEEE Open Journal of the Communications Society* 1 (2020), pp. 957–975. DOI: 10.1109/OJCOMS.2020.3010270.

[5] Mostafa Zaman Chowdhury et al. “Optical Wireless Hybrid Networks: Trends, Opportunities, Challenges, and Research Directions”. In: *IEEE Communications Surveys Tutorials* 22.2 (2020), pp. 930–966. DOI: 10.1109/COMST.2020.2966855.

[6] Alain R. Ndjiongue et al. “Analysis of RIS-Based Terrestrial-FSO Link Over G-G Turbulence With Distance and Jitter Ratios”. In: *Journal of Lightwave Technology* 39.21 (2021), pp. 6746–6758. DOI: 10.1109/JLT.2021.3108532.

[7] Alain R. Ndjiongue et al. *Performance Analysis of RIS-Based nT-FSO Link Over G-G Turbulence With Pointing Errors*. 2021. DOI: 10.48550/ARXIV.2102.03654. URL: https://arxiv.org/abs/2102.03654.

[8] Liang Yang et al. "Free-Space Optical Communication With Reconfigurable Intelligent Surfaces". In: (Nov. 2020).

[9] Narendra Vishwakarma and Swaminathan R. "Performance analysis of hybrid FSO/RF communication over generalized fading models". In: *Optics Communications* 487 (2021), p. 126796. ISSN: 0030-4018. DOI: https://doi.org/10.1016/j.optcom.2021.126796. URL: https://www.sciencedirect.com/science/article/pii/S0030401821000468.

[10] Long Huang et al. "Unified Performance Analysis of Hybrid FSO/RF System With Diversity Combining". In: *Journal of Lightwave Technology* 38.24 (2020), pp. 6788–6800. DOI: 10.1109/JLT.2020.3018125.

[11] Emna Zedini, Hamza Soury, and Mohamed-Slim Alouini. "On the Performance Analysis of Dual-Hop Mixed FSO/RF Systems". In: *IEEE Transactions on Wireless Communications* 15.5 (2016), pp. 3679–3689. DOI: 10.1109/TWC.2016.2524685.

[12] Liang Yang, Wang Guo, and Imran Shafique Ansari. "Mixed Dual-Hop FSO-RF Communication Systems Through Reconfigurable Intelligent Surface". In: *IEEE Communications Letters* 24.7 (2020), pp. 1558–1562. DOI: 10.1109/LCOMM.2020.2986002.

[13] Abir Touati et al. "On the effects of combined atmospheric fading and misalignment on the hybrid FSO/RF transmission". In: *Journal of Optical Communications and Networking* 8.10 (2016), pp. 715–725. DOI: 10.1364/JOCN.8.000715.

[14] I.S. Gradshteyn and I.M. Ryzhik. "Table of Integrals, Series, and Products". In: (2007). URL: http://fisica.ciens.ucv.ve/~svincenz/TISPISGIMR.pdf.

[15] *The Wolfram Functions Site*. Wolfram Research. 1996. URL: https://functions.wolfram.com/HypergeometricFunctions/MeijerG.

[16] Haibo Wang et al. "Performance of Wireless Optical Communication With Reconfigurable Intelligent Surfaces and Random Obstacles". In: *CoRR* abs/2001.05715 (2020). arXiv: 2001.05715. URL: https://arxiv.org/abs/2001.05715.

[17] Proakis. *Digital Communications 5th Edition*. McGraw Hill, 2007.

[18] Ertugrul Basar. “Transmission Through Large Intelligent Surfaces: A New Frontier in Wireless Communications”. In: *2019 European Conference on Networks and Communications (EuCNC)*. 2019, pp. 112–117. DOI: 10.1109/EuCNC.2019.8801961.

[19] M. Chiani, D. Dardari, and M.K. Simon. “New exponential bounds and approximations for the computation of error probability in fading channels”. In: *IEEE Transactions on Wireless Communications* 2.4 (2003), pp. 840–845. DOI: 10.1109/TWC.2003.814350.

[20] “Performance of Multichannel Receivers”. In: *Digital Communication over Fading Channels*. John Wiley & Sons, Ltd, 2004. Chap. 9, pp. 311–635. ISBN: 9780471715221. DOI: https://doi.org/10.1002/0471715220.ch9. URL: https://onlinelibrary.wiley.com/doi/abs/10.1002/0471715220.ch9.

[21] Ehab Salahat and Ali Hakam. “Novel unified expressions for error rates and ergodic channel capacity analysis over generalized fading subject to AWGGN”. In: *2014 IEEE Global Communications Conference*. 2014, pp. 3976–3982. DOI: 10.1109/GLOCOM.2014.7037429.

[22] Antonio Jurado-Navas et al. “A Unifying Statistical Model for Atmospheric Optical Scintillation”. In: *Numerical Simulations of Physical and Engineering Processes*. Ed. by Jan Awrejcewicz. Rijeka: IntechOpen, 2011. Chap. 8. DOI: 10.5772/25097. URL: https://doi.org/10.5772/25097.

[23] Theodoros A. Tsiftsis et al. “Multihop Free-Space Optical Communications Over Strong Turbulence Channels”. In: *2006 IEEE International Conference on Communications*. Vol. 6. 2006, pp. 2755–2759. DOI: 10.1109/ICC.2006.255196.